Colloid Polym Sci (2009) 287:189–201
DOI 10.1007/s00396-008-1966-z

ORIGINAL CONTRIBUTION

Synthesis and characterisation of coating polyurethane cationomers containing quaternary ammonium alkyl groups derived from built-in alkyl bromides

Bożena Król · Piotr Król

Received: 19 September 2008 / Revised: 7 November 2008 / Accepted: 7 November 2008 / Published online: 29 November 2008

Abstract Polyurethane cationomers were synthesised in the reaction of 4,4′-methylenebis(phenyl isocyanate) with polyoxypropylene glycol (M=450) and N-methyl diethanolamine. Amine segments were built-in to the urethane–isocyanate prepolymer in the reaction with 1-bromoalkanes (C_2–C_{10}), and then they were converted to alkyl-ammonium cations. The obtained isocyanate prepolymers were then extended in the aqueous medium. That yielded stable aqueous dispersions which were applied on the surfaces of test poly (tetrafluoroethylene) plates. After evaporation of water, the dispersions formed thin polymer coatings. ^{1}H and ^{13}C NMR spectral methods were employed to confirm chemical structures of synthesised cationomers. Based on ^{1}H NMR and IR spectra, the factors κ and α_1 or α_1 were calculated, which represented the polarity level of the obtained cationomers. The differential scanning calorimetry method revealed decline of T_g for the hard urethane and urea segments from 60 °C to 46 °C when the number of carbon atoms increased in the alkyl radical attached to the ammonium cation. Changes were discussed in the surface free energy (SFE) and its components, as calculated independently according to the methods suggested by van Oss-Good and by Owens–Wendt, in relation to chemical structures of cationomers. The growing length (from C_2 to C_{10}) of the alkyl radical attached to the N atom in the cationomer chain was found to reduce the value of SFE of the polymer coating from 46 to 28 mJ/m^2. That is caused by gradual weakening of long-range interactions, within which the highest share is taken by dispersion interactions.

B. Król · P. Król (✉)
Department of Polymer Science, Faculty of Chemistry,
Rzeszów University of Technology,
Al. Powstańców Warszawy 6,
35-959 Rzeszów, Poland
e-mail: pkrol@prz.rzeszow.pl

Keywords Polarity of bonds · ^{1}H and ^{13}C NMR · IR spectroscopy · Surface free energy parameters by van Oss-Good and Owens–Wendt methods · Mechanical properties · Glass transition temperature

Introduction

As we presented with more detail in our earlier papers [1, 2], PU cationomers are produced chiefly in the reaction of isocyanate-capped prepolymers and low molecular weight tertiary amines which contain hydroxyl groups in their structures. More and more outlets are found for those polymers, inter alia because of their interesting photochemical properties [3]. Another example for that was presented in [4], where the synthesis method, characterization, and photochemical properties of a new polyurethane cationomer with anthracene chromophore groups attached to quaternary ammonium units (PUC–AN) were provided. That cationomer was compared to a model compound (AN) obtained with the use of N-methyldiethanol amine and 9-chloromethylanthracene, in DMF as a solvent. It was synthesised in the quaternisation reaction of urethane polymer and 9-chloromethylanthracene. Polyurethane was obtained from poly(tetramethylene oxide) diol (average MW=2000), tolylene-2,4- and 2,6-diisocyanates (80:20), N-methyldiethanol amine, and terephthalaldehyde-bis(3-hydroxymethylphenylimine), at the molar ratio of 1:3:1:1.

The fluorescence spectra of the anthracene structure indicate that the synthesized compounds present different shifts in solution and in the solid state. The photo-physical investigations revealed that such structures can function as fluorescent chemosensors in the presence of various transition metal ions (UO_2^{+2}, Fe^{3+}, Cu^{2+}). The fluorescence-quenching mechanisms for PUC-AN cationomers and the

proper model compound are attributed to electron and/or energy transfer processes.

Also, the presence of ionic segments improves mechanical and thermal properties of coatings and elastomers obtained from polyurethane cationomers. Novel PUs containing the pyridine moieties were synthesized by the chain extension reaction of isocyanate-endcapped prepolymers with *N,N*′-bis (2-hydroxyethyl) isonicotinamide. The pyridine moieties in the PUs were then chemically cross-linked with the use of short-chain divalent quaternisation agents. The polyurethane cationomers were characterized by spectral, thermal, and mechanical analyses. Spectral results confirmed the quaternisation of tertiary nitrogen, which lead to cross-linking. Compared to conventional PUs, the cross-linked PU networks exhibited improved thermal stability. The damping value (i.e., tan δ) for cationomers was improved over a broad temperature range when compared to conventional PUs [5].

The paper [6], in turn, illustrates the importance of cationic groups within hard segments for the shape memory effect in segmented polyurethane (PU) cationomers. The shape memory polyurethane (SMPU) cationomers were synthesized from poly(ε-caprolactone) (PCL), 4,4′-methylenebis (phenyl isocyanate) (MDI), 1,4-butanediol (BDO), and *N*-methyldiethanolamine (NMDA) or *N,N*′-bis(2-hydroxyethyl) isonicotinamide (BIN). The relations between the structure and the shape memory effect were investigated for the two series of cationomers with various ionic group contents. It was observed that the stress at 100% elongation was reduced for these two series of PU cationomers with increasing ionic group contents. Especially for NMDA series, the stress reduction was more significant. The fixity ratio and recovery ratio of the NMDA series can be improved simultaneously by the insertion of cationic groups within hard segments, but not for the BIN series. Characterizations with differential scanning calorimetry (DSC) and dynamic mechanical analysis methods suggest that the crystallisability of soft segments in SMPU cationomers was enhanced by incorporation of ionic groups into hard segments, leading to a relatively high degree of soft segment crystallization; compared with the corresponding nonionomers, incorporation of charged ionic groups within hard segments can enhance the cohesion force among hard segments, particularly at a high ionic group content [6].

The present paper follows the interest which we have shown up to now and reflected in our earlier papers [1, 2]: it discusses the synthesis of cationomers in which amine segments were built-in to the urethane–isocyanate prepolymer in the reaction with 1-bromoalkanes (C_2–C_{10}), and then they were converted to alkyl-ammonium cations. The obtained isocyanate prepolymers were then extended in the aqueous medium. The produced aqueous dispersions were used to prepare thin polymer coatings, and our attention was fixed on studying the effects of cationomer chemical structures on physical–mechanical properties and surface properties of such resultant polymer coatings.

Experimental

Raw materials and reagents

4,4′-Methylenebis(phenyl isocyanate; MDI) (*M*=250.25 g/mol) was from Aldrich. The reagent was used as purchased.

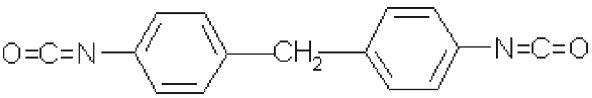

(1)

Polyoxypropylene glycol (M_n≈450 g/mol), (Rokopol 7P) from Chemical Factory "Rokita S.A." in Brzeg Dolny (Poland), (that product was dried under vacuum in nitrogen, at 120°C, during 2 h).

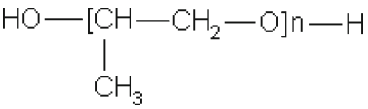

(2)

N-Methyldiethanolamine (*N*-MDA) (M=119.16 g/mol) (Aldrich)

$$(HO - CH_2 - CH_2)_2 > N - CH_3 \quad (3)$$

Bromoethane (*M*=106.97 g/mol) (Aldrich)

$$CH_3 - CH_2 - Br \quad (4)$$

1-Bromobutane (*M*=137.02 g/mol) (Aldrich)

$$CH_3 - (CH_2) - Br \quad (5)$$

1-Bromohexane (*M*=165.08 g/mol) (Aldrich)

$$CH_3 - (CH_2)_5 - Br \quad (6)$$

1-Bromodecane (*M*=221.19 g/mol) (Aldrich)

$$CH_3 - (CH_2)_9 - Br \quad (7)$$

Method for the synthesis of urethane cationomers

Cationomers were synthesised in the glass stand composed of: three-necked flask, heating bowl, mechanical agitator, dropping funnel, thermometer, reflux condenser and nitrogen supply nozzle.

As stage 1, urethane-isocyanate prepolymer was synthesised in the reaction of selected diisocyanate (B), Rokopol 7P (A) and *N*-methyldiethanolamine (X):

$$A + X + 3B \rightarrow BABXB \quad (8)$$

About 10 g (0.04 mol) of diisocyanate were dissolved in 30 cm^3 of THF heated up to 50 °C. Then, 1.5 g (0.0033 mole) Rokopol 7P and 3.93 g (0.0033 mole) *N*-methyl-diethanolamine was added to that solution over about 10 min (Table 1).

Since the amine component (DMPA) was present in the mixture from the very beginning, the reaction proceeded relatively quickly at 50 °C: the final content of groups –NCO was obtained as soon as after 30 min in practice. Hence, there was no need to use any catalyst. The content of –NCO groups in the mixture after that stage amounted to about 0.3 wt.%.

At stage 2, the prepolymer was again reacted with *N*-methyldiethanolamine:

$$n\ \mathrm{BABXB} + n\ \mathrm{X} \rightarrow -(\mathrm{XBABXB})_n- \tag{9}$$

Tertiary amino groups were incorporated into the chains in that way. In order to do that, the selected amine was added to the flask with the prepolymer BABXB in it, at 50 °C, and the flask was maintained at that temperature over 30 min. After that time, the analysed content of –NCO groups was close to 0%.

Alkylammonium cations were produced at stage 3 by alkylation of tertiary amino groups from DMPA with alkyl bromides RBr:

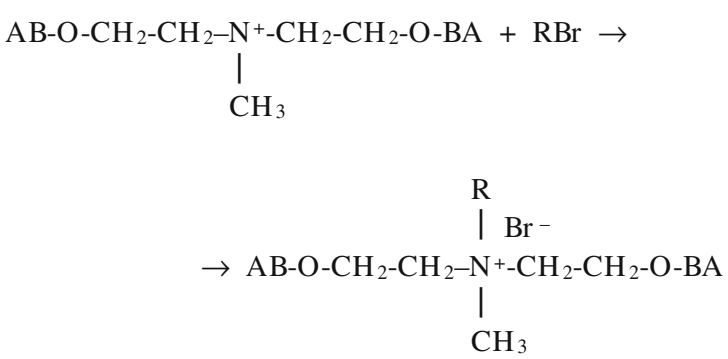

(10)

where:$R = C_nH_{2n+1}$ for n=2, 4, 6 and 10.

The number of moles of RBr (0.0363 mol) to be added to the mixture was adjusted to correspond to the number of moles of built-in tertiary amine contained in the known amount of polymer. The mass fraction of NR^+ groups in so synthesised cationomers resulted from the stoichiometry. The reaction with RBr was conducted at 20 °C during 3 h, and then it was allowed to continue at ambient temperature during 24 h.

At stage 4, redistilled water was added under intensive agitation conditions. That stage was intended not only to produce the dispersion; cationomer chains with the residual –NCO groups were subjected to extension at the same time in the reaction between groups –NCO and water:

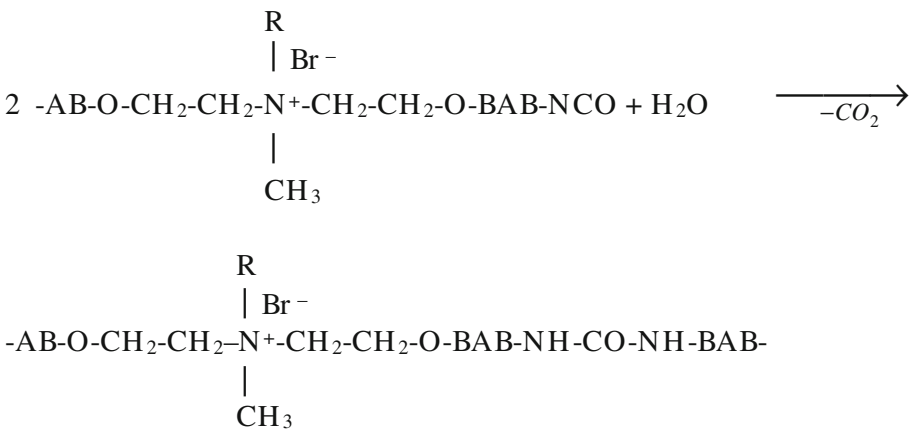

(11)

where:$R = C_nH_{2n+1}$ for n=2, 4, 6 and 10.

The polymer content in the obtained dispersions amounted to about 30 wt.%.

The polymer coatings for further tests were formed by applying the above-mentioned dispersions to a nonpolar surface of poly(tetrafluoroethylene; PTFE, type TARFLEN)

Table 1 Substrates for synthesised cationomers

Sample no.	Synthesis of isocyanate prepolymer, type BABXB (stage 1)			First propagation	*N*-alkylation by RBr	Dispergation and second propagation (stage 4)
	Substrates					
	Type of diisocyanate (B)	Type of polyol (A)	Dihydroxylamine (X)	Stage 2	Stage 3	
0[a]	MDI	Rokopol 7P	–	*N*-MDA	HCOOH[b]	H_2O+HMDA[c]
1			*N*-MDA		C_2H_5Br	H_2O
2					C_4H_8Br	
3					$C_6H_{13}Br$	
4					$C_{10}H_{21}Br$	

[a] Reference sample [1]
[b] In this cationomer, ammonium ions were obtained in the reaction of segments derived from *N*-MDA and HCOOH [1].
[c] 1,6-hexamethylenediamine (HMDA)

and evaporation of water by air-drying at 20 °C. The coatings were then subjected to seasoning under such conditions over 10 days.

Determination of −NCO group content

That determination involved a well-known method, and dibutylamine was used in the tests. Excess of unreacted amine was titrated with the HCl solution, and bromophenol blue was used as an indicator.

NMR spectroscopy

^{1}H and ^{13}C-NMR spectra of the obtained polymers were taken with the use of the spectrometer FT NMR *Bruker Avance 500*^{II}. The samples of coatings (i.e., produced cationomers) were dissolved in DMSO-d_6/h-DMSO, and the solutions with the concentration of about 0.2 g/dm^3 were prepared. TMS was used as a standard [1, 2].

IR spectroscopy

IR spectra were taken with the spectrophotometer Paragon 1000 FT-IR, within 4,000–6,500 cm^{-1}, with the use of ATR technique (the polymer film was placed between the prism walls. The obtained spectra were presented as the relation of transmittance [%] versus wavenumber $\bar{\nu}$[cm^{-1}] [2].

Determination of mechanical properties of coatings synthesised from polyurethane cationomers

The samples with dimensions of 60×10×0.3 mm were submitted to tensile tests. Strength tests of the samples were carried out with the use of a testing machine type Fp-100 from Heckert (Germany), in accordance with the standard procedure [7]. The sample holder travel speed was 500 mm/min, and the measurements were taken over the distance of 25 mm. What was recorded was tensile force versus sample tensile strain. That relation was plotted as a function of tensile stress versus sample elongation.

Tensile strength (TS_b) in MPa was calculated from the formula:

$$TS_b = \frac{F_b}{d \cdot b} \tag{12}$$

where:

F_b force recorded at rupture, [N],
b width of measured length, [mm],
d thickness of measured length, [mm].

Elongation at break (E_b) in % was calculated from the relation:

$$E_b = \frac{L_b - L_0}{L_0} \cdot 100\% \tag{13}$$

where:

L_b length measured at rupture, [mm],
L_o initially measured length, [mm].

DSC analysis

Cationomers obtained from the synthesis process, in the form of polymer film, were analysed by DSC method. Determination of T_{g2} for rigid urethane–urea segments involved the use of the differential calorimeter DSC from *Mettler Toledo, type 822*^{e}. The measurements were taken in the second heating cycle, after the samples had been cooled down to −50 °C.

Method for determination of components of surface free energy for solids

Physical parameters of surface energy of a solid γ_S were found in the present study on the basis of the van-Oss-Good

and Owens–Wendt methods. The van-Oss-Good model assumes that the free surface energy $\gamma_{S,L}$ may be presented as a sum of two components [8, 9]:

$$\gamma_{S,L} = \gamma_{S,L}^{LW} + \gamma_{S,L}^{AB} \tag{14}$$

where:

γ_S^{LW} surface energy connected with long-range interactions (dispersion, polar and induction interactions),

γ_S^{AB} surface energy connected with acid–base interactions, as results from the Lewis theory.

Eq. 14 is generally applicable both to a solid, marked with the subscript S, and to a wetting liquid (standard liquid or tested liquid), marked with the subscript L.

Let us use the symbol γ_S^+ for the component of γ_S^{AB} which is responsible for the free surface energy of the Lewis acid, and the symbol γ_S^- for the component representing the Lewis base. On the basis of the Berthelot theory, which assumes that interactions between molecules of different bodies located on a surface are equal to the geometric mean of interactions between molecules within each of those bodies, one can now formulate the following relations [8, 9]:

– for bipolar substances (liquids and surfaces of solids), which can be equivalent to synthesised PU ionomers—present in the form of aqueous dispersions or coatings:

$$\gamma_S^{AB} = 2\left(\gamma_i^+\gamma_i^-\right)^{0.5} \tag{15}$$

– for nonpolar liquids and surfaces of solids (diiodomethane and PTFE):

$$\gamma_i^{AB} = 0 \tag{16}$$

(where: i=S—solid, L—liquid).

The surface free energy (SFE) parameters for solids (S) and for liquids (L) interacting with those solids should satisfy the equation of van-Oss-Good:

$$\left(\gamma_S^{LW}\gamma_L^{LW}\right)^{0.5} + \left(\gamma_S^+\gamma_L^-\right)^{0.5} + \left(\gamma_S^-\gamma_L^+\right)^{0.5} = \gamma_L(1+\cos\Theta)/2 \tag{17}$$

where Θ is the experimentally found wetting angle between a liquid drop and a solid surface under investigation. So, wetting angles Θ were first measured for the surfaces of cationomer coatings with the use of three model liquids (water, diiodomethane and formamide) with known parameters of γ_L, γ_L^{LW}, γ_L^+ and γ_L^- (Table 6), and then Eq. 15 was used to calculate the values of γ_S^{LW}, γ_S^+ and γ_S^- for the studied cationomers. The values of γ_S^{AB} were calculated from the Eq. 15, while the values of γ_S, from Eq. 14.

Physical parameters of SFE of a solid (γ_S) were found additionally in the present study on the basis of the Owens–Wendt model [10].

The model assumes that the surface free energy γ_S of the solid state may be presented as a sum of two components:

$$\gamma_S = \gamma_S^d + \gamma_S^p \tag{18}$$

where:

γ_S^d surface free energy connected with long-range dispersion interactions (dispersion, polar and induction interactions),

γ_S^p surface free energy connected with polar interactions,

Taking into account the components of SFE in the meaning as it was described above, Owens and Wendt proposed an equation that establishes the relation between the SFE parameters of the standard liquids (L) and of the investigated solid surface (S):

$$\gamma_L\frac{1+\cos\Theta}{2} = \left(\gamma_S^d\gamma_L^d\right)^{0.5} + \left(\gamma_S^p\gamma_L^p\right)^{0.5} \tag{19}$$

where Θ is the experimentally found contact angle between a liquid drop and a solid surface under investigation.

In order to find as well as to validate the values of SFE (γ_S) and the components γ_S^d and γ_S^p of SFE, two sets of standard liquids (water–formamide and diiodomethane–formamide) were used for the investigation of the anionomer surface. The standard liquids have known values of γ_S and remarkably different values of the components γ_S^d and γ_S^p (Table 5). By solving the set of Eq. 19 for the given pair of standard liquids, the γ_S^d values for cationomer coatings were calculated.

The angles Θ were measured with the use of the method suggested by Zisman [11], i.e., by means of optical goniometer (Cobrabid Optica—Warsaw) with a digital camera installed in axial extension of its lens. The liquid drops with the constant volume (about 3–5 μdm^3) were applied to the surfaces of studied samples with the use of a special micropipette. The samples were fixed on the stage of the goniometer. The measurements were taken at 21±1 °C. The values of wetting angles were found from the geometric analysis of pictures taken for liquid drops, which involved the use of the original software developed by Kontrast (Pasłęk, Poland) for interpretation of the Young's equation. The measuring errors for angles Θ come from two sources. The first of them results from different shapes of liquid drops placed on the investigated coatings and from possible interactions between the standard liquid and that subgrade, as well as from different liquid vaporisation rates observed when the pictures were taken. Nine (9) drops were analysed each time which were placed on the surface simultaneously. Another source of potential errors is inaccuracy in graphical interpretation of the pictures with the use of the computer

software. For each picture recorded (i.e., for each liquid drop), the geometrical shape analysis was repeated ten (10) times: the extreme values were rejected, and the arithmetic mean value was calculated for the accepted findings. The measured values of wetting angles and the components of the surface free energy for the cationomer coatings as derived from those measurements were presented in Table 7.

$$-(A-B-X-B)_n-$$

A =

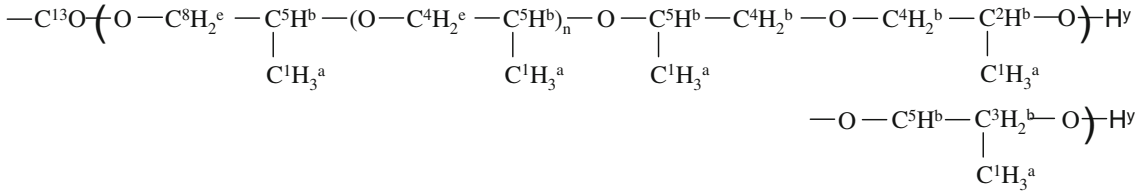

B_1 =

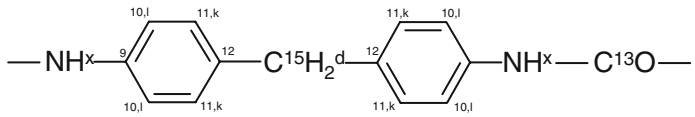

X=

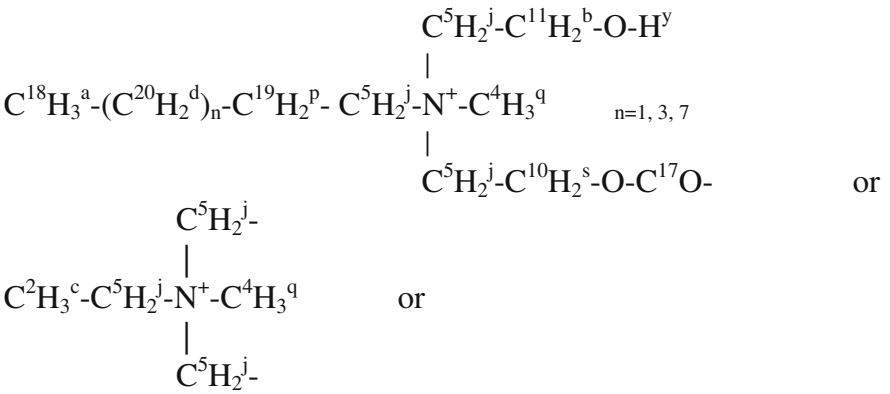

In case of the presence of the not totally reacted N-MDA:

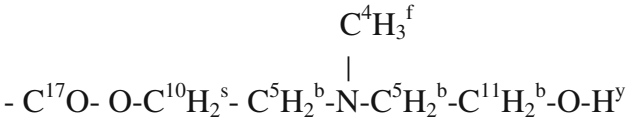

In case of the presence of the not totally reacted RBr:

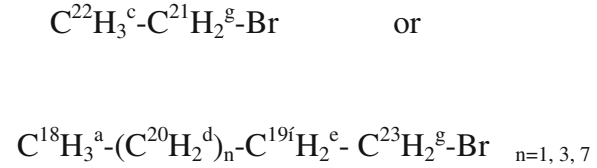

Fig. 1 Chemical structures of polyurethane cationomers

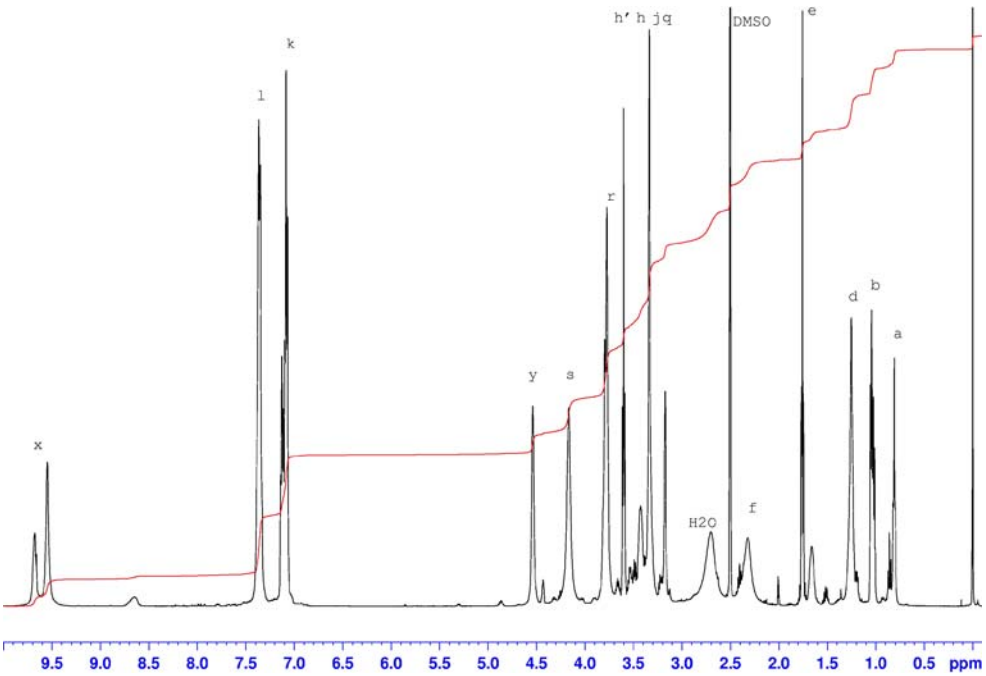

Fig. 2 ^{1}H NMR spectrum of cationomer no. 3 synthesised with MDI diisocyanate, Rokopol 7p, *N*-MDA and $C_6H_{13}Br$

Results and discussion

Chemical structure of cationomers

The chemical structures of the synthesised cationomers were verified on the basis of ^{1}H and ^{13}C NMR spectra. Figure 1 shows structural fragments which make the polymer chains of those cationomers. The exemplary ^{1}H and ^{13}C NMR spectra for cationomer no. 3 were presented in Figs. 2 and 3, while the detailed interpretations for the spectra of all the analysed cationomers were provided in Table 2. The NMR spectra of the synthesised cationomers were composed of exactly the same signals, while essential differences were observed in signal integration of ^{1}H NMR, which makes a proof for diversified amounts of built-in segments (Table 3).

Typical signals of H_k, H_l, C12, C13, C14 and C15 occur in recorded spectra; they represent aromatic rings of MDI, urethane group H_x and C17, which form rigid urethane segments in polyurethanes. Also, the signals are visible for

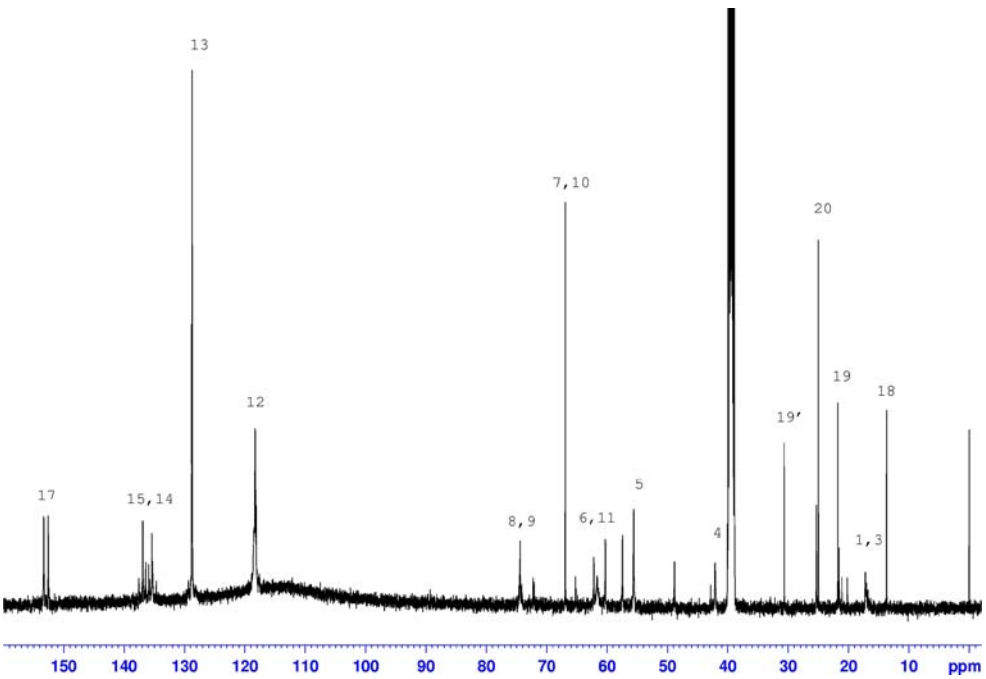

Fig. 3 ^{13}C NMR spectrum of cationomer no. 3 synthesised with aromatic diisocyanate MDI, Rokopol 7p, *N*-MDA and $C_6H_{13}Br$

protons H_a H_b, groups CH_2 and CH, and carbon atoms C1, C6 and C8, which are derived from the structures of polyoxypropylene glycol (Rokopol 7P). Conversion of Rokopol 7P with MDI is "documented" by the signals of protons H_s in group CH_2 bond to the urethane group, and carbon atoms C10. The presence of Rokopol 7P which has not been completely bonded to the polyurethane chain may be evidenced by the signal of proton H_y and confirmed by the presence of the signal for carbon atom C7. The fact that *N*-MDA was built-in and converted in the reaction with alkyl bromides into quaternary alkyl-ammonium cations is documented by the signals H_j, H_q, H_p and H_s, as well as C4, C5, C8 and C10. Incomplete conversion of *N*-MDA may not be ruled out here, which could be evidenced by the signals H_y and C11. Those signals, however, are not unequivocal since they may represent unconverted Rokopol 7P as well (signal C6). In general, there is no unequivocal evidence for possible alkyl bromides C2, C4, C6 and C10 which have not been incorporated into polyurethane chains, which would certainly be disadvantageous. The most characteristic signals for unconverted RBr, i.e., C21 and C23 are absent, while the signal for protons H_g is not unequivocal in this case—as can be seen in Table 2. It is interesting in this context that the signal H_q of the group N^+–CH_3 is more clearly outlined in the spectra of cationomers nos. 3 and 4, and additionally the signal H_f is absent which is specific for that group in unconverted amine *N*-MDA.

Some additional information may be derived when the successive integration ratios I_a/I_r are compared to I_b/I_r, i.e., when the signals coming successively from H_a and H_b are referred to those for the protons H_r (Table 3). It becomes

Table 2 Interpretation of NMR spectra for polyurethane cationomers

Type of nucleus	Sample No			
	1	2	3	4
Fig. 1	^{1}H NMR			
a	–	0.88–0.91	0.81–0.87	0.83–0.87
b	1.01–1.06	1.01–1.06	1.01–1.06	1.01–1.06
c	1.74–1.77	–	–	–
d	–	1.15–1.36	1.18–1.36	1.19–1.27
e	–	1.74–1.77	1.73–1.77	1.72–1.79
p	–	–	1.6608	1.493–1.666
f	2.29	2.29	2.32–2.40	2.236–2.45
DMSO	2.50	2.50	2.50	2.50
H_2O in DMSO	2.67	2.66–2.68	2.70	2.88
h, h′, j, q	3.34–3.77	3.16–3.79	3.17–3.79	3.14–3.80
r	3.77	3.77	3.77	3.77
s	4.13–4.15	4.13–4.15	4.17	–
y	4.43–4.53	4.43–4.53	4.43–4.54	4.55
k	7.06–7.13	7.06–7.14	7.07–7.14	7.08–7.14
l	7.33–7.36	7.32–7.36	7.35–7.36	7.32–7.39
x	9.53–9.64	9.53–9.65	9.55–9.68	9.53–9.83
Fig. 2	^{13}C NMR			
18	–	13.41	13.69	13.86
1,3	17.0–17.2	17.20	16.78–17.20	16.52–17.20
19	–	19.07	20.18–21.80	20.21–22.01
20	25.03 impurity	25.02	25.03–25.33	25.04–25.70
19′	–	–	30.65	28.06–31.17
4	42.19	42.19	42.84	42.91
DMSO+C16	40.5	40.5	40.5	40.5
5	55.69	55.67; 57.44	55.58; 57.46	55.00; 57.48
6,11	61.75	60.32; 61.73	60.31–62.20	60.33–62.20
7,10	66.92	65.23; 66.92	65.23; 66.92	65.24; 66.93
8,9	72.08–74.56	74.44	72.06–74.41	72.11–74.43
12	118.20–118.28	118.18; 118.28	117.67–118.30	118.09–118.39
13	128.72	128.71; 128.81	128.72; 128.75	128.82
14	134.74; 135.4	134.73–135.34	134.67–135.38	134.61–135.84
15	136.98; 137.57	135.96–137.56	135.91–137.59	136.52–137.66
17	153.41	152.60; 153.40	152.60–153.33	152.62–152.92

apparent that more and more *N*-MDA was built-in to successive cationomers 1–4, at the cost of Rokopol, which was not intentional anyway. The growing value of the integration ratio I_d/I_r is unequivocally representative for the increasing number of apolar groups CH_2 in relation to urethane structures derived from MDI, which is consistent with the expectations.

So, one may declare that the recorded spectra confirm the general structures of chains in synthesised cationomers, which makes it possible to use signal integrations in ^{1}H NMR spectra in a more extensive structural analysis.

That analysis involved comparison of polarities of obtained cationomers, on the basis of the parameter κ which was defined especially for that purpose. That parameter was calculated from the values of integrated signals in ^{1}H NMR spectra. The protons were distinguished which represented polar and apolar structural fragments which formed the chains of cationomers.The factor κ was calculated in the way which was analogous to that defined in [1, 2]:

$$\kappa = \frac{I_P}{I_P + I_N} \cdot 100\% \tag{20}$$

where:

$$I_P = \sum \left(I_h + I_{h'} + I_j + I_q + I_s + I_y + I_x\right) \tag{21}$$

makes the sum of signals recorded over a wide band of δ= 3.0–5.0 ppm (designated as h, h′) from groups CH_2 and CH connected to polar ether groups present in Rokopol soft segment, signals *j* from N^+–CH_2 and *q* from N^+–CH_3 groups, and signals s from CH_2 groups connected directly to urethane groups. The signals *y* were also considered which represented incompletely converted groups –OH, and so were the signals *x* of polar groups NH in urethanes, urea compounds and allophanates (*x*, *q*).

The sum of integrations of signals generated by apolar structures:

$$I_N = \sum \left(I_a + I_b + I_c + I_e + I_d + I_f + I_p + I_r + I_k + I_l\right) \tag{22}$$

covers the signals within δ=0.8–2.45 ppm, coming from protons in groups CH_3 of Rokopol, alkyl bromides and unreacted *N*-MDA (designated as a, b, c and f), and internal groups CH_2 (designated as d, e and p). The signals were also included for the bridge group CH_2 in MDI diisocyanate (*r*) (δ=3.77 ppm) and signals for aromatic protons in MDI (*k*, *l*).

With that assumption, Eq. 21 presents the value which is proportional to the amounts of chemical structures with the dominant effect on polar interactions, and Eq. 22 represents nonpolar interactions in the structures of synthesised cationomers (Fig. 2). One may assume then that the value of the factor κ as calculated from Eq. 20 makes the physical characterisation of the polarity degree of a given cationomer. The data presented in Table 3 show that the values of the factor κ for the series of synthesised cationomers vary within 33.45–40.88%. Those values are much lower than those determined by us earlier for cationomers synthesised from MDI, Rokopol 7P and *N*-MDA, for which HCOOH was the ammonium-cation-forming component, and for which κ= 46.3–46.6% [1]. For the need of comparison, it is worth mentioning that the factor κ (which was determined in the same way) for the series of cationomers synthesised with the use of *N*-MDEA, HCOOH and various diisocyanates (MDI, TDI, HDI, IPDI and HMDI) varied within 39–50%, and the highest values of κ were found for the cationomers synthesised from aromatic diisocyanates TDI and MDI [2]. The analysis of the values for the factor κ as provided in Table 3 reveals that the observable reduction in polar interactions appears not earlier than for cationomer no. 4 which has been synthesised with the use of 1-bromodecane. For the need of comparison, the value of that factor, calculated exactly in the same way, for sample no. 0 (Table 1) amounted to κ=50.58, which makes the evidence for considerably higher polarity of the cationomer obtained from MDI, Rokopol 7P and HCOOH and forming ammonium cations. Hence, *N*-alkylation of cationomers improves noticeably the hydrophobic performance of the coatings; that should also be reflected by their surface free energy values.

Table 3 Analysis of signal integration in NMR spectra of synthesised cationomers

Sample no.	1	2	3	4
	Integration (conventional unit)			
$I_h + I_{h'}$	1.0325	1.2903	1.9024	1.9566
I_j				
I_q				
I_s	0.8865	0.8216	0.5613	0.6632
I_y	0.0624	0.1441	0.3182	0.2584
I_x	0.4663	0.4909	0.5100	0.6151
I_P	2.4477	2.7469	3.2919	3.4933
I_a	–	0.1006	0.2998	0.5233
I_b	0.4236	0.3899	0.4460	0.3995
I_c	0.4950	–	–	–
I_d	–	0.2011	0.5780	2.2523
I_e	–	–	0.3111	0.4440
I_f	0.6645	0.6178	0.4211	0.2177
I_p	–	–	0.1760	0.3330
I_r	0.5405	0.6208	0.8112	0.7721
I_k	1.0225	1.0423	1.024	1.0077
I_l	1.000	1.000	1.000	1.000
I_N	4.1461	3.9725	5.0672	6.9496
κ [%]	37.12	40.88	39.38	33.45
I_a/I_r	0	0.162	0.370	0.678
I_b/I_r	0.784	0.628	0.550	0.517
I_d/I_r	0	0.324	0.713	2.917

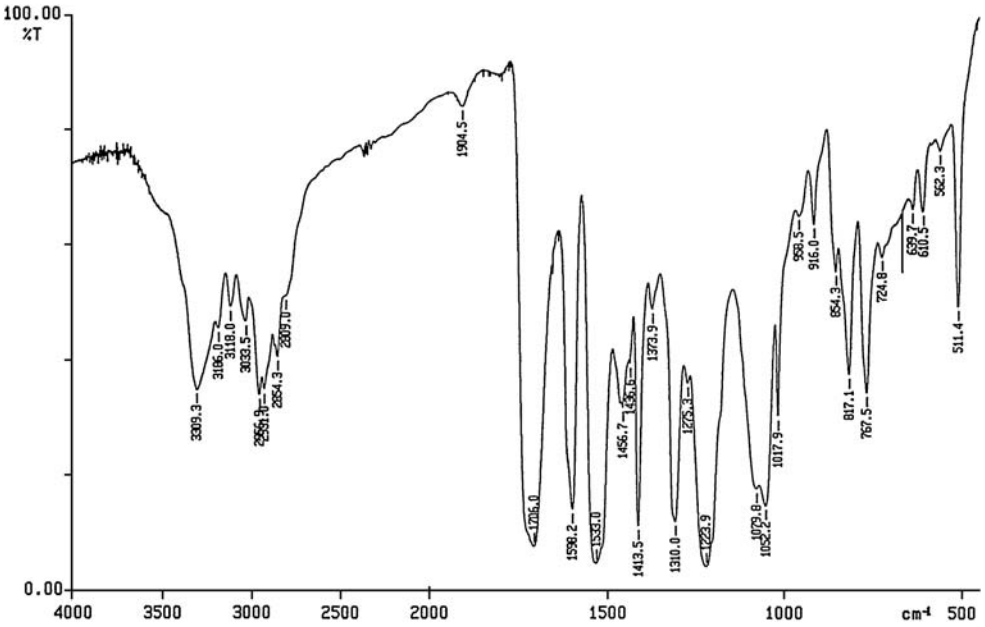

Fig. 4 IR spectrum of cationomer no. 3

The above conclusion is also confirmed by IR spectroscopic tests. The ratios α_1 and α_2 calculated on the basis of IR spectra:

$$\alpha_1 = \frac{A_{CO}}{A_{CH_3+CH_2}} \tag{23}$$

$$\alpha_2 = \frac{A_{CO}}{A_{CH_2\ scissoring}} \tag{24}$$

were adopted as the additional criterion for evaluation of polarity of chemical structures of synthesised cationomers (The values of A_{CO}, A_{CH2} and A_{CH3} in the Eqs. 23 and 24 represent absorbance data for bands of groups CO, CH_2 and CH_3, respectively, as defined in accordance with the Lambert-Beer first law). Deformation bands of the groups CH_3 (symmetrical and anti-symmetrical) as well as CH_2 (scissoring bands; Fig. 4) may be expected within 1,372–1,465 cm^{-1}. So, it is more convenient to determine the total absorbance $A_{CH3\ +\ CH2}$ and take it as the reference for absorbance of valence vibrations of the polar carbonyl groups in urethane and urea structures (α_1 factor). After having assumed, irrespective of the above, that the band at 1,457 cm^{-1} corresponds exclusively to scissoring vibrations of CH_2 group in the studied cationomers, the analogous factor of α_2 was additionally calculated (Table 4).

One may conclude from the observed reduction in the values of both those factors that the successive cationomers under consideration—in accordance with our expectations—will have lower and lower relative shares of carbonyl groups, which is decisive for the strength of polar interactions. Hence, the potential number of hydrogen bonds drops down as they need the involvement of carbonyl group oxygen atoms. Incorporation of longer and longer alkyl groups into cationomer chains should therefore yield cationomers which are more and more hydrophobic.

Like parameter κ, the declining values of factors α_1 and α_2 confirm the expected reduction in polar interactions in macromolecules of studied cationomers.

Table 4 Analysis of absorbance values of selected IR spectra for synthesised cationomers

Sample no.	1	2	3	4
Valence vibration of CO group $\overline{\nu}$, cm^{-1}	1,725.1	1,720.6	1,706.0	1,700.4
A_{1725} (conventional scale)	0.9922	1.3074	1.1166	0.2508
Bending vibrations of CH_3 and CH_2 groups	$\Delta\nu = 1,372 - 1,465\ cm^{-1}$			
$A_{CH_3+CH_2}$ (conventional scale)	1.2849	1.7803	1.7535	0.5959
CH_2 scissoring vibrations $\overline{\nu}$, cm^{-1}	1,456.4	1,459.5	1,456.7	1,457.0
$A_{CH_2 scissoring}$ (conventional scale)	0.2823	0.4434	0.4964	0.1318
$\alpha_1 = \frac{A_{co}}{A_{CH_3+CH_2}}$	0.7700	0.7344	0.6368	0.4209
$\alpha_2 = \frac{A_{co}}{A_{CH_2 scissoring}}$	3.5147	2.9486	2.2494	1.9029

Mechanical properties and glass transition temperature of polyurethane coatings

The weaker intermolecular interactions in the analysed cationomers, as observed in structural studies, may be expected to result in inferior mechanical strength of coatings prepared from those materials. That was confirmed by the values measured for tensile strength, with simultaneous increase in elongation at the break observed (Table 5). A quantum jump decrease of tensile strength value from about 9 to 3.5 MPa and a clear increase of elongation at break from 60% to 200% were noticed for sample no. 3, which was obtained with the use of 1-bromohexane as the quaternisation-reacting substance. That should be explained by the plasticization effects of hexyl and decyl groups which reduce intermolecular interactions between hard urethane or urea segments which are present in cationomer chains. Those effects are not so evident for ethyl and butyl groups.

Another important parameter, which characterises mechanical–thermal properties of polymer coatings, is the glass transition temperature T_g. Two temperature values are usually specific for polyurethane elastomers: they represent vitrification of flexible segments $T_{g1}<0$ and of rigid segments $T_{g2}>0$. Table 5 provides the values of T_{g2} for urethane and urea hard phases present in the studied cationomers. The plasticization effect is more and more noticeable for successive cationomer samples, which shows up as gradual decrease of T_{g2} from 66 °C down to 40 °C.

Surface free energy of the coating obtained from polyurethane cationomers

The known parameters γ_L, γ_L^{LW}, γ_L^+ and γ_L^- for model fluids were utilised in the calculations of SFE, and they are presented in Table 6.

Table 7 provides the values of wetting angles Θ as found, and also, components of surface free energy calculated on the basis of those angles in accordance with the van Oss-Good and Owens–Wendt methods, for coatings obtained from the studied polyurethane cationomers.

The collected data show that *N*-alkylation of obtained cationomers with the use of 1-bromoalkanes reduces the surface free energy of the coatings obtained from those materials, in relation to the coating prepared from the cationomer material produced with the use of HCOOH (sample 0). The values of γ_S go gradually down to about 26 mJ/m^2 for the cationomer involving $C_{10}H_{21}Br$, while noticeable reduction in SFE takes place even for cationomer no. 2 which was produced with the use of C_4H_9Br. The values of γ_S, calculated form van Oss-Good and Owens–Wendt methods, are close to each other, although the Owens–Wendt method yields somewhat higher SFE values. Correctness of this approach is confirmed by very close values of SFE as obtained from calculations based on two pairs of model measuring fluids: water–formamide and formamide–diiodomethane (Table 7).

The findings from the van Oss-Good method bring us to the conclusion that the basic impact on the value of γ_S comes from the γ_S^{LW} component of long-range interactions. However, the values of acid–base interactions γ_S^{AB} cannot be evaluated precisely, and these should be estimated as maximum about 3 mJ/m^2, with the dominant contribution from base interactions γ_S^-.

The analysis of Owens–Wendt method findings suggests, on the other hand, that dispersion interactions γ_S^d prevail within the long-range interactions, which gradually weaken when nonpolar structures derived from 1-bromoalkanes are introduced. The share held by polar interactions γ_S^p is generally small: based on calculations for the system of water–formamide model fluids, their value does not exceed $\gamma_S^p = 2 - 4.5\,\mathrm{mJ/m^2}$, and it is not dependent (like the value of γ_S^{AB}) on the structure of the ammonium cation NR_4^+ which is present in the synthesised cationomer. It should be mentioned that the molar fractions for alkylammonium cations were similar in the considered cationomers 1–4 (Table 1). The structural effects in the analysed cations on their FSE values and on the values of the FSE components are—as one can see—much more complex, and they may not be directly correlated with solely structural parameters of polarity as found by the NMR (κ) and IR (α_1 or α_2) methods, although the trends in so determined structural parameters are in line with those in calculated SFE values. Thus, our further studies will be aimed at developing more complex correlations for those values.

Table 5 Mechanical properties and glass transition temperature for cationomer coating

Sample no.	E_b (%)	TS_b (MPa)	T_{g2} (°C)
1	63	10.14	65.5
2	58.7	9.02	59.1
3	214	3.63	56.7
4	294	3.41	40.8

Table 6 Surface properties of model measuring liquids [16]

Model measuring fluid	Free surface energy parameters (mJ/m^2)		
	γ_L	γ_L^d	γ_L^p
Water	72.8	21.8	51
Formamide	58.0	39.0	19.0
Diiodomethane	50.8	48.5	2.3

Conclusions

Our research demonstrated that the use of C_2–C_{10} 1-bromoalkanes as alkyl-ammonium cation-forming compounds makes it possible to produce stable dispersions of waterborne polyurethane cationomers in the polyaddition process of MDI, polyoxypropylene glycol ($M_n \approx 450$ g/mol) and *N*-methyl-diethanolamine, which is organised in a few stages. Those dispersions, after application to the PTFE substrate and evaporation of solvent(s), form coatings with gradually declining polarities. The NMR and IR spectral methods were employed to confirm the expected structures of those cationomers. Based on integrated ^{1}H NMR signals, the parameter κ was calculated which had been defined just for that purpose and which characterises the degree of polarity for the synthesised cationomers. The analogous parameters α_1 and α_2 were determined based on the analysis of absorbances for some selected bands in IR spectra.

When bigger and bigger alkyl groups are introduced to cationomers, which adds to plasticization of synthesised polyurethanes, it becomes visible through lower glass transition temperatures of rigid urethane–urea segments, T_2, from 66 °C to 40 °C. However, there is a disadvantageous effect as well, i.e., drop in tensile strength from about 9 to 3.5 MPa and the accompanying increase of elongation at break, from 60% up to 200%.

As expected, the introduced structural changes result in weaker long-range interactions in synthesised cationomers, which is responsible for lower values of surface free energy of polymer coatings produced from those cationomers. The studies of FSE by the van Oss-Good and Owens–Wendt methods, based on wetting angles, revealed that the total values of γ_S for the tested coatings went down from about 40 to 26 mJ/m^2. Hence, these materials may be considered low-polarity ones against generally polar performance of polyurethane coatings (>40 mJ/m^2). On the contrary, the apolar coating of PTFE, type TARFLEN, used in this study as a substrate for coatings, has the energy of γ_S=21.8 *m*J/m^2 [12]).

Based on the findings from the van Oss-Good method, one may conclude that the basic effect on the value of γ_S comes from the component γ_S^{LW} of long-range interactions, while the findings from the Owens-Wendt method calculation show that the dispersion interactions γ_S^d play the dominant role here. The values of acid–base interactions γ_S^{AB}, however, may not be determined precisely, and these should be estimated as maximum at about 3 mJ/m^2, with the dominant contribution from base interactions γ_S. Polar interactions, as per Owens–Wendt method, should be estimated as $\gamma_S^p = 2 - 4.5\,\mathrm{mJ/m^2}$, and—alike acid–base interactions γ_S^{AB}—they are independent in practice on the cationomer structure.

Our research revealed that the effects of chemical structures in polyurethane cationomers on the values of their FSE and its components is complex, and those effects could not be simply correlated at the present stage of our studies with polarity parameters coming from NMR (κ) and IR (α_1 or α_2) methods, although the trends in changes of so determined structural parameters and in calculated SFE values are the same.

The described method of the synthesis makes it possible to obtain new coating materials based on the polyurethane cationomers with reduced free surface energy what may be used to produce waterproof protective coatings for ceramic materials and is a part of promising direction for obtaining new biomedical materials hardly undergoing biodegradation after grafting into alive organism and used for example to make coatings reconstructing membranes of the internal organs damaged during diseases or accidents [13–15].

Table 7 Experimental values of contact angles and parameters of FSE as calculated by Owens–Wendt and van Oss–Good methods for cationomer coatings

Sample no.	Contact angles Θ (°)						Water–formamide			Formamide–CH_2I_2			Water–Formamide–CH_2I_2				
	Model measuring fluids						Parameters of FSE (mJ/m^2)										
							by Owens–Wendt method						by van Oss–Good method				
	CH_2I_2	SD	Formamide	SD	Water	SD	γ_S^d	γ_S^p	γ_S	γ_S^d	γ_S^d	γ_S	γ_S^{LW}	γ_S^-	γ_S^+	γ_S^{AB}	γ_S
0	31.5	1.7	52.5	1.4	68.7	1.6	Not analysed						38.10	12.33	0.20	3.22	43.49
1	30.00	1.33	60.00	1.17	82.96	0.79	43.937	1.927	45.9	45.338	0.111	45.4	41.54	4.08	0	0	41.5
2	48.38	0.15	68.30	0.17	80.31	0.24	34.131	4.560	38.7	35.256	0.367	35.6	30.74	9.72	0.004	0.39	31.1
3	57.78	0.25	68.28	0.16	85.89	0.48	35.834	2.398	38.2	35.248	0.371	35.6	26.09	4.72	0.52	3.14	30.4
4	61.81	0.18	80.53	0.24	80.53	0.11	24.028	4.341	28.4	28.656	0.000	28.7	24.06	8.07	0	0	24.0

References

1. Król P, Król B (2008) Colloid Polym Sci 286:1111
2. Król P, Król B (2008) Colloid Polym Sci 286:1243
3. Buruiana EC, Melinte V, Buruiana T, Simionescu BC (2005) J Appl Polym Sci 96:385
4. Buruiana EC, Olaru M, Simionescu BC (2007) Eur Polym J 43:1359
5. Sriram V, Radhakrishnan G (2005) Polym Bull 255:165
6. Zhu Y, Hu J, Yeung K-W, Choi K-F, Liu Y, Liem H (2007) J Appl Polym 103:545
7. PN-EN ISO 527
8. Good JR (1991) In: Lee LH (ed) Fundamentals of adhesion. Dekker, New York, p 153
9. Żenkiewicz M (2006) Polimery 51:169 and 51:584
10. Owens DK, Wendt RC (1969) J Appl Polym 13:1741
11. Zisman WA (1964) Ad Chem Am Chem Soc 43:1
12. Król P, Król B (2006) J Eur Ceramic Soc 26:2241
13. Park JH, Bae YH (2002) Biomaterials 23:1797
14. Górna K, Gogolewski S (2002) Polym Degrad Stab 75:113
15. van Minnen B, Stegenga B, van Leeuwen MBM, van Kooten TG, Bos RRM (2006) J Biomed Mater Res 76A:377
16. Dann JR (1970) Coll Interf Sci 32:302